

# Cortical and Subcortical Mechanisms of Brain-Machine Interfaces

Silvia Marchesotti <sup>1,2,3</sup> Roberto Martuzzi,<sup>1,2,4</sup> Aaron Schurger,<sup>1,2,5,6</sup>  
Maria Laura Blefari,<sup>1,2,5</sup> José del R. Millán,<sup>2,5</sup> Hannes Bleuler,<sup>3</sup> and  
Olaf Blanke <sup>1,2,7\*</sup>

<sup>1</sup>Laboratory of Cognitive Neuroscience, School of Life Sciences, Ecole Polytechnique Fédérale de Lausanne, Geneva, Switzerland

<sup>2</sup>Center for Neuroprosthetics, Ecole Polytechnique Fédérale de Lausanne, Geneva, Switzerland

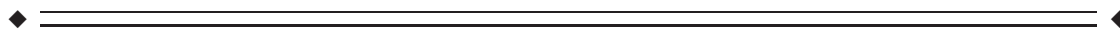
<sup>3</sup>Laboratory of Robotic Systems, School of Engineering, Ecole Polytechnique Fédérale de Lausanne, Lausanne, Switzerland

<sup>4</sup>Fondation Campus Biotech Geneva, Geneva, Switzerland

<sup>5</sup>Defitech Chair in Brain-Machine Interface, School of Engineering, Ecole Polytechnique Fédérale de Lausanne, Geneva, Switzerland

<sup>6</sup>Cognitive Neuroimaging Unit, NeuroSpin Research Center, INSERM, Gif-Sur-Yvette, France

<sup>7</sup>Department of Neurology, University Hospital, Geneva, Switzerland



**Abstract:** Technical advances in the field of Brain-Machine Interfaces (BMIs) enable users to control a variety of external devices such as robotic arms, wheelchairs, virtual entities and communication systems through the decoding of brain signals in real time. Most BMI systems sample activity from restricted brain regions, typically the motor and premotor cortex, with limited spatial resolution. Despite the growing number of applications, the cortical and subcortical systems involved in BMI control are currently unknown at the whole-brain level. Here, we provide a comprehensive and detailed report of the areas active during on-line BMI control. We recorded functional magnetic resonance imaging (fMRI) data while participants controlled an EEG-based BMI inside the scanner. We identified the regions activated during BMI control and how they overlap with those involved in motor imagery (without any BMI control). In addition, we investigated which regions reflect the subjective sense of controlling a BMI, the sense of agency for BMI-actions. Our data revealed an extended cortical-subcortical network involved in operating a motor-imagery BMI. This includes not only sensorimotor regions but also the posterior parietal cortex, the insula and the lateral occipital cortex. Interestingly, the basal ganglia and the anterior cingulate cortex were involved in the subjective sense of controlling the BMI. These results inform basic neuroscience by showing that the mechanisms of BMI control extend beyond sensorimotor cortices. This knowledge may be useful for the development of

Contract grant sponsors: Roger de Spoelberch Foundation, the Bertarelli Foundation, Centre d'Imagerie BioMédicale (CIBM) of the University of Lausanne (UNIL); Contract grant sponsor: AS was supported in part by ERC Starting Grant 640626.

\*Correspondence to: Olaf Blanke, EPFL SV BMI LNCO, Campus Biotech, Ch. des Mines 9, CH-1202 Genève, Switzerland. E-mail: olaf.blanke@epfl.ch

Received for publication 23 September 2016; Revised 28 February 2017; Accepted 3 March 2017.

DOI: 10.1002/hbm.23566

Published online 21 March 2017 in Wiley Online Library (wileyonlinelibrary.com).

---

BMIs that offer a more natural and embodied feeling of control for the user. *Hum Brain Mapp* 38:2971–2989, 2017. © 2017 Wiley Periodicals, Inc.

**Key words:** brain-machine interface; EEG-fMRI; motor imagery; sense of agency

---

## INTRODUCTION

Brain-machine interfaces (BMIs) enable the voluntary control of external devices through real time decoding of neural signals. Exploiting either invasive [Carmena et al., 2003; Fetz, 1969; Hochberg et al., 2012] or non-invasive techniques [Leeb et al., 2013; Wolpaw and McFarland, 2004], BMIs translate patterns of brain activity into command signals bypassing the biological corticospinal motor pathways. In non-invasive BMIs, brain patterns are mainly recorded using electroencephalography (EEG) while users are engaged in a cognitive task, such as motor imagery (MI). This has been defined as a dynamic state during which a subject simulates an action mentally without any body movement [Decety, 1996]. In MI-based non-invasive BMIs (>300 research reports according to PubMed) users typically imagine performing repeated right or left hand movements resulting in discriminable patterns that are used to drive binary decisions (e.g., right-left movements of a cursor or other devices) [Millán et al., 2010; Wolpaw et al., 2002]. In this case, the most commonly used feature is  $\mu/\beta$  band suppression over sensorimotor regions [McFarland et al., 2000; Neuper et al., 2006; Pfurtscheller and Lopes da Silva, 1999], as these modulations are strongly associated with both contralateral motor execution and MI. A linear classifier is typically used to discriminate these spectral EEG signatures in real-time and translate them into a command signal.

Although the rapid evolution of brain-controlled systems has led to a growing interest in the brain mechanisms involved in BMI control, relatively few animal and human studies have directly investigated the changes in brain activity associated with the operation of a BMI [Jarosiewicz et al., 2008; Koralek et al., 2012]. Recent studies have confirmed that fronto-parietal and subcortical oscillations, involved in sensorimotor and visuo-motor processing, are also recruited during learning to control a BMI [Miller et al., 2010; Wander et al., 2013]. However, these studies were not able to address the distributed brain mechanisms involved in BMI control as they did not provide full-brain coverage (as is possible with functional magnetic resonance imaging [fMRI]). Although a number of studies exploiting the advantages of fMRI have investigated different aspects of BMI control, results were limited since no real-time feedback was provided to the participants [Halder et al., 2011; Ninaus et al., 2013].

EEG-based BMI control inside of an MRI scanner combines the advantages of real-time BMI control and the high temporal resolution of EEG with the high spatial resolution

and whole brain coverage offered by fMRI. However, this approach presents significant technical challenges, which have hampered attempts to exploit this technique. To date only two studies successfully investigated the BOLD fMRI signal while participants controlled an EEG-based BMI. Hinterberger et al. [2005] used a BMI paradigm (based on slow cortical potentials) and found strongest activation in the SMA and premotor cortex during a self-regulation task as compared to the rest condition. In addition, subcortical modulations in the basal ganglia and thalamus were associated with either a positive or a negative shift in the self-regulated slow cortical potential. In a recently published study, Zich et al. [2015] investigated the relationship between the EEG signals and the BOLD response while subjects controlled a MI-based BMI inside the MRI scanner with and without feedback. These authors reported a negative correlation between the power in the  $\mu$ -band and the BOLD signal in premotor cortex contralateral to the imagined hand movement, and a stronger activation associated with the visual feedback. However, this analysis was limited to premotor cortices and did not investigate modulation outside these areas, that is, what is the network involved in MI-based BMI control at the full-brain level. Furthermore, these studies neglected an important aspect of real and imagined actions, which is the subjective feeling of being in control over the movement (i.e., the sense of agency [SoA]), recently investigated for “BMI actions” in a behavioral study [Evans et al., 2015].

In the present study, we developed an EEG-BMI setup that is MRI compatible, allowing us to record fMRI data while human subjects controlled a fully functioning MI-based EEG BMI in the scanner. We had three main goals for this study, each one with an associated hypothesis. First, we wanted to identify the regions active during BMI-control, and we expected to find activation in a broader network than the one described in earlier work (i.e., beyond sensorimotor cortex). Second, we wanted to assess via a meta-analysis the regions that are consistently active during MI and compare these with those active during BMI-control. We anticipated that there would be a marked overlap between activations during the present BMI task and MI. Finally, we sought to investigate the neural correlates of the SoA without the contribution of somatosensory reafference. As in a previous study on the SoA for BMI actions [Evans et al., 2015], we manipulated the visual feedback while subjects were engaged in a cursor control task. We expected to find an overlap with brain regions having been associated with agency for bodily movement [David et al., 2008], as well as regions specific for BMI-mediated action.

## MATERIALS AND METHODS

### Participants

Sixteen healthy participants (2 females and 14 males, mean age 25.5 years,  $SD \pm 2.7$ , range 22–32) took part in the experiment, which was approved by the Ethics Committee of the Faculty of Biology and Medicine of the University of Lausanne and was conducted in accordance with the Declaration of Helsinki. The 16 participants were selected from an initial pool of 36 subjects, based on their ability to control a BMI assessed during a recruiting session performed outside the scanner.

### Experimental Procedure

#### Participant recruiting session

The recruiting session was aimed at selecting high aptitude BMI users who would take part in the BMI-fMRI session. During the recruiting session, participants had to kinesthetically imagine clasping either the left or right hand to control the movement of a cursor, similar to many BMI systems based on the spontaneous modulation of the sensorimotor rhythm (SMR) [Pfurtscheller et al., 1997; Wolpaw and McFarland, 2004]. Previous studies have shown that changes in the subject's posture, from sitting to a reclined position, can influence brain activity due to the effects of baroceptive signaling [Lipnicki, 2009; Rice et al., 2013]. Therefore, to mimic the situation that would later be encountered in the MRI scanner, the recruiting session was conducted with the participants laying supine and viewing the visual stimuli (presented on a video display) through a 45° inclined mirror placed in front of their eyes. The session consisted of two parts: during the first part (off-line) participants performed two runs of MI without visual feedback. During each run of 40 trials, subjects were asked to imagine clasping either the left or the right hand. The EEG signal was recorded from 28 electrodes located over the sensorimotor cortex (see section "EEG signal acquisition and BMI" for further details). The data were then used to compute a set of spatial filters (common spatial patterns [CSP], [Blankertz et al., 2008; Guger et al., 2000]) as well as the coefficients for a binary linear classifier able to discriminate between the two imagined directions. The classifier computed during this first training phase was used in the second part of the session for the on-line control of the cursor, during which the BMI algorithm translated the EEG activity into commands used to drive the cursor. Participants were instructed to use the same MI strategy as in the off-line session to operate the cursor. This session comprised two runs of 32 trials; each trial ended when the cursor reached the cued edge of the screen, or after 6 s, whichever came first.

Only subjects with a mean BMI performance above chance in the recruiting session were retained to take part into the BMI-fMRI session (see section "BMI-control related

measurements" for details regarding the method used to obtain the chance threshold). BMI performance was measured by considering which direction the classifier had output the majority of the time within one trial.

#### BMI-fMRI session

**Setup.** During the BMI-fMRI session, participants laid supine in the MR scanner holding a button response pad in each hand, while the EEG signal was simultaneously acquired. Visual stimuli were projected onto a translucent screen positioned at the end of the bore and subjects looked at it through an inclined mirror attached to the head coil.

**Stimuli.** The experiment included two off-line and two online runs. As in the recruiting session, the experiment began with the off-line runs, during which the subject performed MI without visual feedback while the EEG signal was recorded. No fMRI data were acquired during the off-line runs. This step was required to compute the spatial filters (CSPs) and classifier parameters to be used during the fMRI recording session.

After the initial motor-imagery task and off-line classifier training, the subject had a short break during which an anatomical MRI scan was acquired and then the on-line testing session began. During this session, the visual feedback was presented in the form of a rectangular cursor that moved toward the left or right side of the screen depending on the classifier output. On half of the trials, the visual feedback was experimentally manipulated by reversing the direction of the cursor movement (*deviated* trials). Therefore, the online runs included four experimental conditions arranged in a  $2 \times 2$  factorial design with cue direction (left/right) and feedback manipulation (*undeviated/deviated*) as factors. The four experimental conditions were randomly intermixed across trials. There were a total of 64 trials divided into two runs, each comprising eight repetitions per experimental condition. Each trial began with the presentation of a fixation cross (2 s) followed by a central arrow (1 s), pointing either to the left or to the right, indicating the side of the screen toward which the subject should attempt to move the cursor (Fig. 1A). For the next 6 s, the subject was allowed to perform MI and attempt to move the cursor all the way to the cued side of the screen. If the cue reached the side of the screen, then the cursor disappeared and a fixation cross was displayed for the remaining time. At the end of the 6-s, period of cursor control subjects had to report whether or not they had felt in control of the cursor movement by pressing the button on either the right- or left-hand response pad. The specific response hand used was counterbalanced across subjects. The response period (3 s) was followed by 6 s of rest. The total duration of each trial was 18 s (Fig. 1A). The total duration of the BMI-fMRI session was on average 3:30 h, from the subject preparation until the end

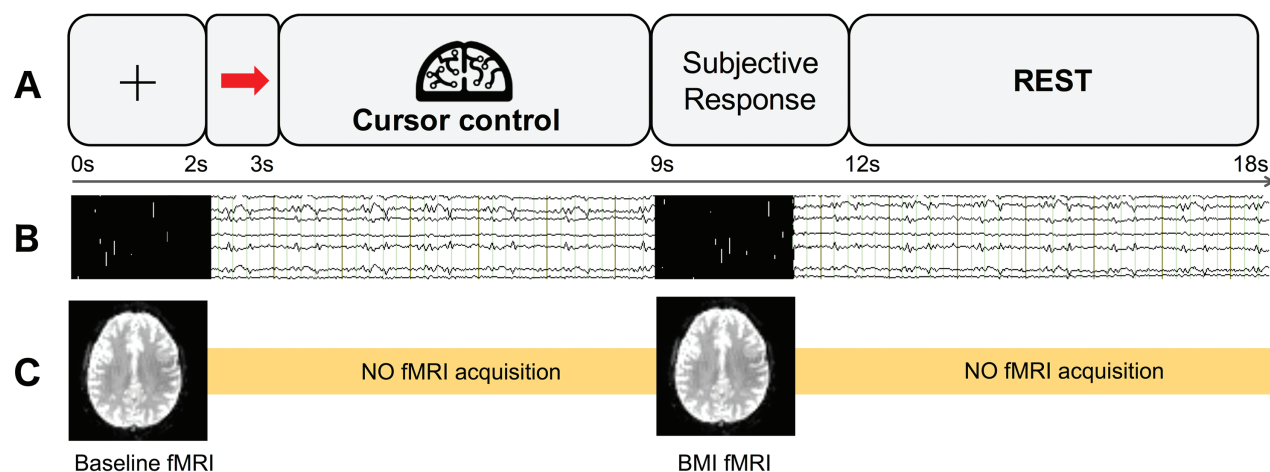


**Figure 1.**

Procedure. **(A)** Experimental paradigm. **(B)** EEG data were recorded for the entire duration of the experiment. **(C)** Two fMRI scans were acquired for each trial, the first during the presentation of a fixation cross and the second after the 6 s of on-line brain-machine interface (BMI) cursor control.

of the fMRI acquisition session. This relatively long duration prevented the acquisition of a greater number of trials.

Two full-brain volumes of fMRI data were acquired per trial, one at the beginning of the trial, simultaneous with the fixation cross, and a second one immediately after the cursor control period, exactly 9 s after the first volume acquisition (Fig. 1C). We chose not to acquire volumes during the cursor control period to avoid compromising the EEG signal quality with an MR gradient artifact. See “Magnetic resonance imaging” section below for further details.

The velocity of the cursor was adjusted for each subject to avoid a premature termination of the trial (the cursor reaching the edge of the screen). This was done to ensure that the subject was performing MI throughout the entire trial, so that the acquisition of the relevant fMRI volume would sample the accompanying brain activity (if the cursor were to reach the edge of the screen too quickly, then the subject might consider the trial as finished and disengage from the task).

### EEG Signal Acquisition and BMI Loop

#### Participant recruiting session

A 64-channel EEG system (g.tec medical engineering GmbH, Graz, Austria) was used for the recruiting session performed outside the scanner. The BMI loop, which refers to the processing chain from the decoding of brain activity to the feedback presentation, used a subset of 28 of the 64 EEG channels. This subset included all the electrodes situated over the sensorimotor cortex, with the exception of C2, C1, and FCz, and also P4, P3, Pz, and Fz. This

particular configuration was imposed by the channel availability in the MR-compatible cap used during the experiment inside the scanner. The ground was located on the forehead and the reference was placed on the right earlobe. During this session, the EEG signal was sampled at 256 Hz.

#### BMI-fMRI session

During the BMI-fMRI session, the EEG signal was acquired using a 64 channel MR-compatible EEG system (BrainProducts GmbH, Gilching, Germany). Electrode AFz was used as the ground and FCz was used as the reference. The raw signals were recorded at 5 kHz using proprietary software (Recorder, BrainProducts), corrected for the magnetic-field-gradient artifact on-line (RecView, BrainProducts), using an approach based on template subtraction [Allen et al., 2000], down-sampled to 200 Hz, and finally sent to a laptop dedicated to on-line classification through Ethernet communication. The maximum delay between one recorded sample and the classifier output was 110 ms. The same 28 channel configuration used in the recruiting session performed outside the scanner was also used for the on-line BMI control.

#### BMI loop

For all BMI sessions, whether inside or outside the scanner, the BMI control loop was based on the CSP algorithm [Blankertz et al., 2008; Guger et al., 2000]. This method comprises two steps: a calibration and a feedback phase.

**Calibration.** The calibration phase uses the EEG data acquired during the offline session to compute the classifier parameters required for the on-line cursor control. First, the EEG data (offline) were visually inspected to discard

trials containing ocular or muscle artifacts. The retained EEG data were band-pass filtered between 8 and 30 Hz, to include the  $\mu$  (8–12 Hz) and  $\beta$  (12–30 Hz) frequency bands, and then used to compute the CSPs for the two classes of imagined movement. The CSP algorithm finds spatial filters (in the same number as the electrodes) that maximize the variance for one class while minimizing the variance for the other class. The variance of the band-pass filtered signal is proportional to the band power of the signal: as MI induces patterns of activity, specific for each of the two imagined direction (i.e., a prominent contribution from electrodes located in the hemisphere contralateral to the imagined direction), the signal variance in the frequency band exploited for the BMI directly reflects the presence of the above mentioned patterns of activity. Based on the projection matrix computed with the CSP method [see for details Guger et al., 2000], the first two CSPs will carry a prominent contribution from one class, while the last two CSPs will account for the other class. The use of these four CSPs to construct the feature vector constitutes a well-established standard in BMI applications, motivated by previous studies indicating four as the optimal number of CSP in a 2-class paradigm [Müller-Gerking et al., 1999]. Lastly, these four subject-specific features were used as the input vector for the linear classifier (LDA classifier).

**Feedback.** In the feedback phase, the EEG data are decoded in real time to control the movement of the cursor on the screen. As during the calibration phase, the EEG data were band-pass filtered in the  $\mu$  and  $\beta$  frequency bands (8–30 Hz) and then projected onto the first and last two CSPs.

The variance across time of this filtered signal was computed and then log-transformed to normalize the signal distribution. Based on the sign of the linear classifier output, at each time step one sample was attributed either to the left or the right-hand class; thus, the cursor position was updated either to the left or to the right relative to the current position. The velocity of the cursor was proportional to the distance of the feature vector from the linear decision boundary and sampled from a range of 10 discrete values for which the sign determines the direction of movement. In the experiments conducted inside the scanner, the visual feedback was manipulated on half of the trials chosen at random. During these incongruent trials (*deviated trials*), the sign of the classifier output was inverted thus reversing the direction of cursor movement with respect to the motor-imagery EEG signal. This was done to experimentally manipulate, in our participants, the subjective feeling of being in control over the cursor movement.

### Magnetic Resonance Imaging

The MRI data were acquired on a 3T Siemens Trio MR system (Siemens Medical, Erlangen, Germany), equipped with a 12-channel coil. Functional images were obtained using an echo-planar imaging sequence (repetition time [TR]=9 s, echo time [TE]=30 ms, field of view

[FoV]=192 mm, flip, angle = 90°) and comprised 36 slices (in-plane resolution  $3 \times 3 \text{ mm}^2$ , thickness 3 mm, gap 0.3 mm) acquired in interleaved order and covering entirely the cerebral hemispheres.

The acquisition of each volume was packed within the first 2 s of the TR, allowing a silent period of 7 s between two consecutive acquisitions. This method, combined with the experimental design, allowed the participant to control the cursor via the BMI control loop using the EEG signal acquired when the scanner was silent. With such a long TR, we acquired two images per trial: the first was acquired during the cue presentation, reflecting the activity during rest; the second was acquired at the end of the cursor control period, reflecting the activity during MI.

During the training of the BMI classifier after the two off-line runs inside the scanner, a sagittal T1-weighted 3D gradient-echo sequence (MP2RAGE) [Marques et al., 2010] was acquired for each subject (160 contiguous sagittal slices, slice thickness 1 mm, matrix size  $240 \times 256$ , FoV = 256 mm, flip angle = 0°, with TE = 2.63 ms, TR = 7.2 ms, T11 = 0.9 s, T12 = 3.2 s, TRmpage = 5 s).

### BMI-Control Related Measurements

To obtain a bias-free estimate of subjects' ability to control the BMI, we computed BMI-control performance using the *area under the curve* (AUC, values range [0-1]). The AUC refers to the area under the *receiver operating characteristic*, here computed by labeling each trial according to the class (right or left) assigned by the classifier for the majority of samples. A hit was assigned if this label matched the cued direction. The AUC offers the advantage of being less affected by a possible classification bias toward one of the two directions. Importantly, this measure is obtained based on the raw classifier output, independently of the presence of the experimental deviation in the cursor trajectory.

Furthermore, to identify which subjects achieved successful BMI-control, we used the binomial cumulative distribution, a method previously proposed to identify the statistical significance threshold for BMI control [Combrisson and Jerbi, 2015; Müller-Putz et al., 2008]. This empirical approach takes into consideration the number of trials performed by the subject, as previous studies pointed out that for a two-class BMI paradigm, the theoretical chance level of 50% only holds for an infinite number of trials [Combrisson and Jerbi, 2015]. In our case, based on the number of trials in our paradigm (32 trials per class), the threshold for statistical significance was found to be around 61% at  $P < 0.05$  (corresponding to an AUC value of  $\sim 0.61$ , assuming the same number of instances of both classes). It is important to note that only subjects whose BMI performance exceeded this threshold during the *participant recruiting session* outside the MRI scanner, were invited to participate in the second session.

During the BMI-fMRI session, subjects had to report at the end of each trial whether or not they had felt in control of the cursor movement, by answering the question: “Did you feel that you were the one controlling the cursor?” The answer (YES/NO) was collected by means of two MRI compatible button pads (Current Designs, Philadelphia, PA), one in each hand. Subjects were instructed to hold the pads in their hands while keeping the palms facing up, throughout the entire duration of the experiment. The association between the answer and the hand used to answer was counterbalanced across subjects to control for motor preparation.

## Data Analysis

### Electrophysiological correlates of MI

To ensure that our subjects were performing MI, we analyzed the EEG signals for signs of suppression of the well-known sensorimotor  $\mu$ -rhythm [Pfurtscheller and Lopes da Silva, 1999], which is associated with MI over the hemisphere contralateral to the imagined hand movement. We used the data collected during the offline session, without visual feedback, and investigated modulations in the  $\mu$ -band power spectrum (event related spectral perturbation, ERSP, [Makeig, 1993]), separately for right and left MI, that is, electrodes C3 and C4, over the last 4 s of a total of 6 s of MI. We discarded the first 2 s since this time window could contain artifacts related to eye movements. We considered as a baseline the first 2 s at the beginning of each trial prior to the MI period, during which we presented the fixation cross and the cue indicating which hand had to be imagined. Separately for each of the two imagined directions, we then compared the  $\mu$ -rhythm over electrodes C3 and C4 and tested (two tailed paired *t*-test) for the presence of significantly stronger power suppression over C3 during right MI and over C4 during left MI.

### Common spatial patterns

The CSPs offer a neurophysiologically meaningful insight into the topographical properties of SMR. Each CSP is a weighted combination of the EEG electrodes, and thus the higher the value assigned to a given electrode, the stronger the contribution of the underlying neural activity in classifying between the two imagined directions. One can expect to find a lateralized peak of activity over the sensorimotor areas, contralateral to the imagined hand movement [Blankertz et al., 2008]. Therefore, as a first step in the analysis of the EEG data, we inspected the CSP computed at the beginning of the experiment in the fMRI. More specifically, we looked at which electrode, of the first and last CSP (Fig. 2) was weighted the most heavily in the classification, expecting it to be found over the hemisphere contralateral to the imagined hand movement.

### BMI performance

We tested whether subjects' performance (AUC) changed between the two sessions (recruiting and BMI control inside the MR scanner), between *deviated* and *undeviated* trials, and between “control” and “no-control” trials (i.e., depending on whether the subject reported feeling him or herself to be in control over the cursor movement). We further investigated the relationship between BMI performance and the reported feeling of control across subjects by computing the correlation between BMI performance and the percentage of trials in which the subject reported feeling in control, separately for *undeviated* and *deviated* trials.

### fMRI data analysis

The fMRI data were pre-processed using SPM8 (Wellcome Department of Cognitive Neurology, London, UK). Of the 16 subjects selected to participate in the fMRI experiment, data from four subjects had to be discarded: three subjects asked to withdraw from the experiment partway through, and the fMRI data for one subject were contaminated with presence of artifacts in the fMRI images, leaving  $N = 12$  subjects. Functional scans were first realigned spatially to the first volume acquired and in time to the first slice acquired. After realignment, volumes were normalized to the Montreal Neurological Institute (MNI) template, resampled to a voxel size of  $3 \times 3 \times 3 \text{ mm}^3$ , and smoothed with an isotropic Gaussian kernel (6 mm full width at half maximum).

Structural volumes were co-registered with the functional volumes, normalized to the MNI template brain, and resampled to a  $1 \times 1 \times 1 \text{ mm}^3$  voxel size.

Two spatial analyses were conducted to investigate the different brain mechanisms underlying the control of a BMI. Active areas during each condition were assessed with a general linear model using the canonical hemodynamic response function as the basis function. Inference at the population level (group analysis) was obtained by means of second-level statistics based on random field theory [Friston et al., 1994].

To investigate the activity elicited by BMI control and by the effect of the congruence of the visual feedback, we performed a  $2 \times 2$  repeated-measures analysis of variance (ANOVA) with “cue direction” (left/right) and “cursor movement manipulation” (*undeviated/deviated*) as within-subject factors.

We first investigated the average brain response to the four experimental conditions regardless of the cue direction and of the movement manipulation ( $q < 0.05$  FDR corrected, 30-voxel cluster threshold) and checked its consistency with the results of a meta-analysis (see “Results” section) of prior MI imaging studies conducted in healthy subjects. Then, differences in BOLD signal intensity related to the cue direction and to the cursor movement manipulation were investigated ( $q < 0.05$  FDR corrected, 30-voxel cluster threshold). Finally, we tested whether activations in those clusters

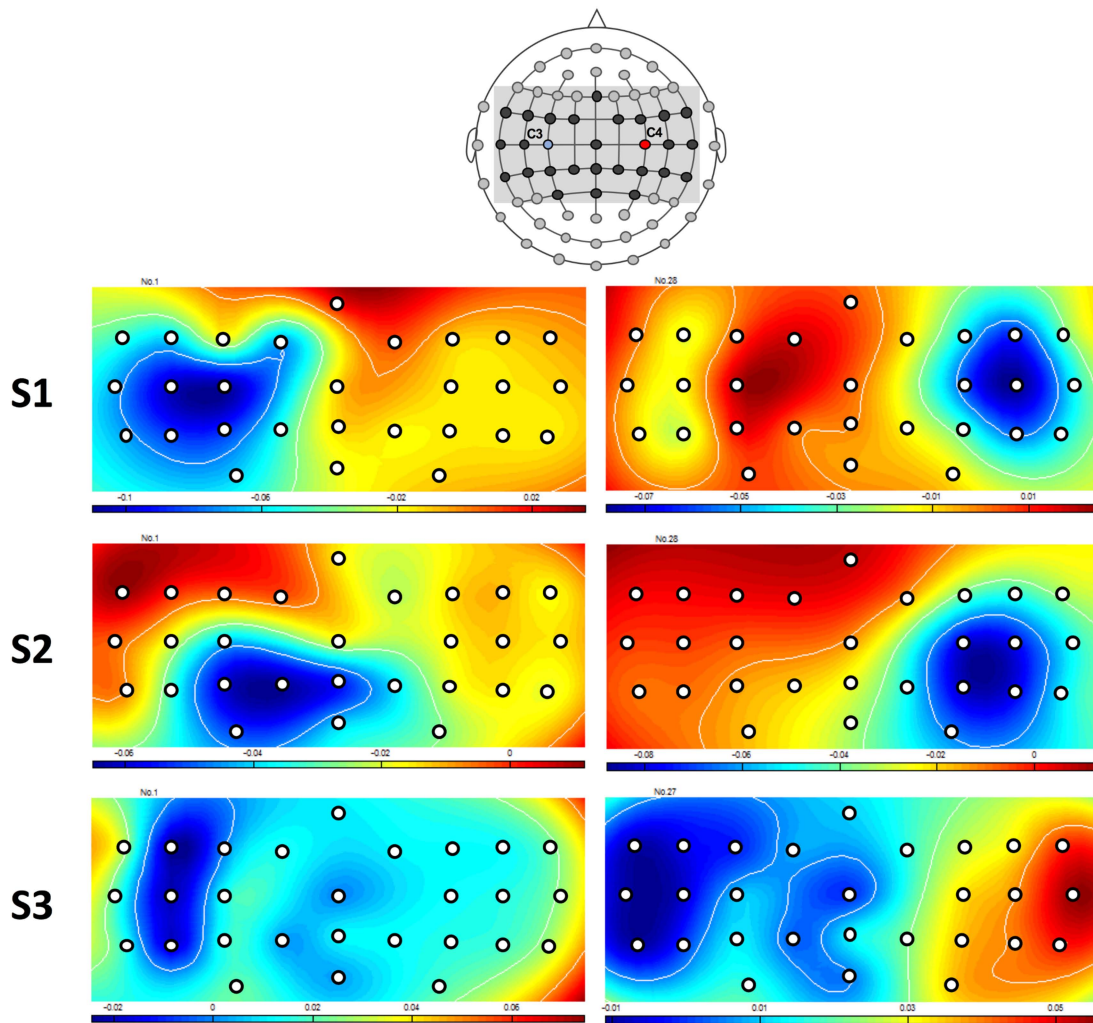


**Figure 2.**

Electrode configuration and Common spatial patterns. (Top) The 28-electrode subset highlighted with white circles is used for BMI loop out of a 64-channel MRI-compatible cap (10–20 configuration). (Bottom) CSP for right and left motor imagery in three representative subjects. Subjects S1 and S2 show the stereotypical patterns of activation associated with motor-imagery based non-invasive BMIs. [Color figure can be viewed at [wileyonlinelibrary.com](http://wileyonlinelibrary.com)]

showed different trends (i.e., activation or deactivation) depending on the cued direction. For each sensorimotor cluster found in the previous analysis, we extracted the mean beta values obtained by contrasting separately the right and left motor-imagery scans against the “rest” scan.

The second analysis investigated which brain areas were involved in the subjective feeling of control over the movement of the cursor. To address this question, we reanalyzed the fMRI data with a 2-way repeated-measures ANOVA, with “cue direction” (left/right) and “feeling of control” (YES/NO) as within-subjects factors. We investigated the brain areas associated with the reported feeling of control by contrasting the “control” versus “no control” trials ( $q < 0.05$

FDR masked with the regions showing a significant response to at least one experimental condition at  $P < 0.001$ , clusters with a spatial extent of at least 30 contiguous voxels).

All clusters were anatomically labeled using the probabilistic cytoarchitectonic maps defined in the SPM Anatomy Toolbox (version 1.8) [Eickhoff et al., 2009].

### Meta-analysis of hand MI studies

We computed a meta-analysis of prior fMRI MI studies conducted in healthy subjects to test the consistency of our results with previous MI studies. The meta-analysis was performed using the BrainMap software (Research

**TABLE I. Neuroimaging studies included in the ALE meta-analysis of neuroimaging studies of hand motor imagery**

Publications	Subjects	Contrast	Number of Locations	Imaging Modality
[Binkofski et al., 2000]	6	Imagery of Somatosensory Guided Movement vs. Rest	6	fMRI
		Imagery of Visually Guided Movement vs. Rest	8	
[Boecker et al., 2002]	6	Sequences I to V Combined > Rest	11	PET
		Sequences I to V Combined < Rest	6	
		Positive correlation with sequence complexity	5	
		Inverse correlation with sequence complexity	5	
[Creem-Regehr and Lee, 2005]	12	Tools > Scrambled Tools, Imagined Grasping	15	fMRI
		Scrambled Tools > Tools, Imagined Grasping	5	
		Shapes > Scrambled Shapes, Imagined Grasping	13	
		Scrambled Shapes > Shapes, Imagined Grasping	9	
		Tools > Shapes, Imagined Grasping	5	
[Decety et al., 1994]	6	Motor Imagery - Visual Inspection	34	PET
		Motor Imagery - Movement Observation	52	
[Ehrsson et al., 2003]	7	Imagined Finger - Imagined Toe Movement	3	fMRI
		Imagined Finger - Imagined Tongue Movement	3	
		(Imagined Finger - Imagined Toe Movement) + (Actual Finger - Actual Toe Movement)	3	
		(Imagined Finger - Imagined Tongue Movement) + (Actual Finger - Actual Tongue Movement)	3	
		Imagined Finger Movement - (Imagined Toe + Imagined Tongue Movement)	3	
		Imagined Toe Movement - (Imagined Finger + Imagined Tongue Movement)	2	
		Imagined Tongue Movement - (Imagined Finger + Imagined Toe Movement)	3	
[Filimon et al., 2007]	15	Imagined Reaching > Passive Viewing	13	fMRI
		Actual Reaching + Observed Reaching + Imagined Reaching	3	
[Gerardin et al., 2000]	8	Motor Imagination vs. Rest	20	fMRI
		Motor Imagination vs. Motor Execution	15	
[Grafton et al., 1996]	7	Imagined Grasping > Object Viewing	12	PET
[Guillot et al., 2009] 9	50	Visual Imagery vs. Passive Listening	34	fMRI
		Kinesthetic Imagery vs. Passive Listening	44	
		Visual Imagery vs. Kinesthetic Imagery	9	
		Kinesthetic Imagery vs. Visual Imagery	18	
[Hanakawa et al., 2008]	13	Finger Tapping, Imagery	12	fMRI
		Finger Tapping, Imagery + Finger Tapping, Movement	18	
		Finger Tapping, Imagery > Finger Tapping, Movement	4	
		Finger Tapping, Imagery > Instructional Cue	10	
[Harrington et al., 2007]	11	Write > Rest	13	fMRI
		Draw > Rest	22	
		Draw > Write	16	
[Johnson et al., 2002]	8	Left Hand Preparation	28	fMRI
		Right Hand Preparation	30	
		Left Hand Grip Selection	7	
		Right Hand Grip Selection	13	
[Jueptner et al., 1997]	12	Imagine vs. Rest	2	PET
[Kuhntz-Buschbeck et al., 2003]	12	Motor Imagery, Simple, Right Hand vs. Baseline	5	fMRI
		Motor Imagery, Complex, Right Hand vs. Baseline	12	
		Motor Imagery, Simple, Left Hand vs. Baseline	7	
		Motor Imagery, Complex, Left Hand vs. Baseline	13	
		Imagery > Execution, Right Hand	4	
		Imagery > Execution, Left Hand	1	
[Lacourse et al., 2005]	54	Novel, Image vs. Rest	16	fMRI
		Skilled, Image vs. Rest	16	
		Novel, Image > Move	2	
		Skilled, Image > Move	5	
		Novel > Skilled, Image	8	

TABLE I. (continued).

Publications	Subjects	Contrast	Number of Locations	Imaging Modality
[Lamm et al., 2007]	17	Reaching Range Predictions/Averaged > Gender Matching	20	fMRI
		Correlation between Reaching Range Prediction > Baseline	6	
[Seitz et al., 2000]	6	Right Finger Imagery	6	fMRI
[Servos et al., 2002]	12	Arm Motor Imagery	2	fMRI
[Stephan et al., 1995]	6	Imagined Movement vs. Motor Preparation	26	PET
		Imagined vs. Executed Movements	3	
[Szameitat et al., 2007a]	15	Imagery > Fixation	11	fMRI
		Imagine Upper Extremity Movements - Fixation	13	
		Imagine Whole Body - Upper Extremity Movements	5	
[Szameitat et al., 2007b]	17	Right - Rest	23	fMRI
		Left - Rest	24	

Abbreviations: fMRI: functional magnetic resonance imaging, PET: positron emission tomography.

Imaging Institute of the University of Texas Health Science Center San Antonio; <http://brainmap.org/> Laird et al. [2009] and in accordance with the methods described by Laird et al. [2005] and modified later by Eickhoff et al. [2009]. A total of 21 fMRI and PET studies (see Table I) involving hand MI tasks were selected from the BrainMap database using the Sleuth software (Sleuth, BrainMap). The peak locations found in these selected studies were then converted into a probabilistic image using dedicated software (GingerALE, BrainMap) using the activation likelihood estimation (ALE) technique. Briefly, the ALE approach works by modeling each focus with a 3D-gaussian probability distribution centered at the given location with a standard deviation inversely proportional to the number of subjects of the study, and then the union of the activation probabilities is computed at each voxel to derive the ALE map of the study [Eickhoff et al., 2009]. We finally tested whether and where the ALE maps were significantly different from zero ( $q < 0.05$  FDR corrected, minimum cluster size of  $100 \text{ mm}^3$ ), indicating a convergence of the results of the selected imaging studies. To test the consistency of the results of our BMI maps with the previous studies on hand MI, we explored the overlap between the results of the meta-analysis and the average brain response to the four experimental conditions obtained with the first ANOVA described above ( $q < 0.05$ , FDR corrected, 30-voxel cluster threshold).

## RESULTS

### EEG Data: Electrophysiological Correlates of MI

The EEG data recorded during the offline part of the recruiting session and during the BMI-fMRI session exhibited a modulation of  $\mu$ -band power that is classically observed during MI. For this, we considered the EEG signal over C3 and C4 separately for each of the two imagined directions and expected a stronger  $\mu$ -band suppression for the electrode located over the contralateral hemisphere with respect to the

imagined direction [i.e., Pfurtscheller and Neuper, 1997]. We observed that the C3 signal exhibited a significantly stronger suppression for rightward cursor control with respect to C4 (two tailed paired  $t$ -test, *recruiting session*:  $t = 2.86$ ,  $P < 0.05$ ; *cursor control inside the scanner*:  $t = 2.47$ ,  $P < 0.05$ , Fig. 3). Similarly, leftward cursor control was associated with a significantly stronger suppression over electrode C4 than over C3 (*recruiting session*:  $t = 4.26$   $P < 0.005$ ; *cursor control inside the scanner*:  $t = 2.45$ ,  $P < 0.05$ , Fig. 3). The analysis of  $\mu$ -band suppression confirmed that we were able to record classical EEG signatures of hand MI during BMI control, even when the EEG data were recorded inside the MRI scanner.

### EEG Data: Common Spatial Patterns

We computed CSP topographies for each experimental session (recruiting session; BMI-fMRI session) based on the training data. Analysis confirmed that the four most discriminant CSPs, two for each imagined direction (extracted from data recorded during both sessions) exhibited the stereotypical patterns of EEG-activity commonly associated with motor-imagery based non-invasive BMIs (Fig. 2) [Blankertz et al., 2008; Guger et al., 2000]. This was found for the majority of our subjects (10 out of 12 subjects). We also extracted the maxima of both the right and left spatial patterns, computed for the recruiting and the BMI-fMRI sessions separately to examine whether the electrode showing the strongest contribution to classification was located over the contralateral hemisphere with respect to the direction of cursor movement in both sessions. This was the case in ten of the twelve subjects tested for the recruiting as well as for the BMI-fMRI session (in the remaining two subjects, both maxima were located over the same hemisphere).

### EEG Data: BMI-Control Performance

Only subjects exhibiting BMI-control performance above the empirical chance threshold (corresponding to an AUC

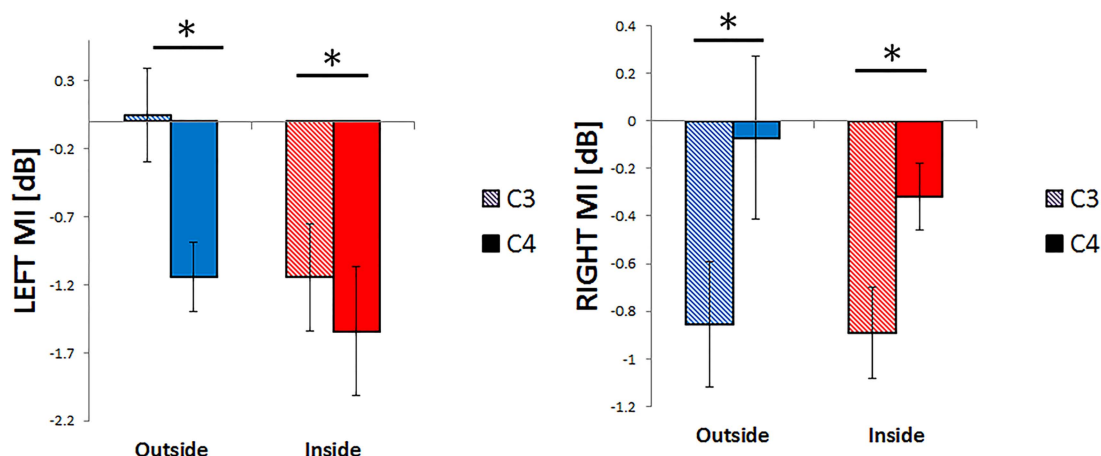


**Figure 3.**

Sensorimotor rhythm suppression. Modulation of  $\mu$ -rhythm suppression over sensorimotor regions during left and right hand motor imagery over electrodes C3 and C4. In both the training session outside the scanner and the cursor control inside the MRI, a statistically significant stronger power suppression is shown over the electrode placed contralateral to the imagined hand movement. [Color figure can be viewed at [wileyonlinelibrary.com](http://wileyonlinelibrary.com)]

value of  $\sim 0.61$ ) during the *training session*, were allowed to participate in the BMI-fMRI session. In this latter session, the majority of our participants (8 out of 12 subjects) did perform above chance (Fig. 4). In particular, in the session inside the MRI scanner, we observed a high variance in performance, ranging from 0.5 to 1. Furthermore, comparing participants' performance between the two sessions revealed a significant decrease in performance during the session performed inside the fMRI scanner (two-tailed paired *t*-test,  $t = 3.15$ ,  $P < 0.01$ ). This decrease is likely due to the discomfort of the MRI environment reported by some of our

subjects and that lead to two subjects withdrawing from the experiment part way through. This decrease is comparable with the drop in performance inside the MRI scanner recently reported by Zich et al. [2015].

However, unlike this previous study, in our experiment the average BMI control performance across subjects was found to be above chance during both sessions (training session:  $0.89$ ,  $SD \pm 0.11$ , BMI-fMRI session:  $0.78$ ,  $SD \pm 0.19$ ).

Significant difference in AUC was observed neither between *deviated* and *undeviated* trials nor between "control" and "no control" trials.

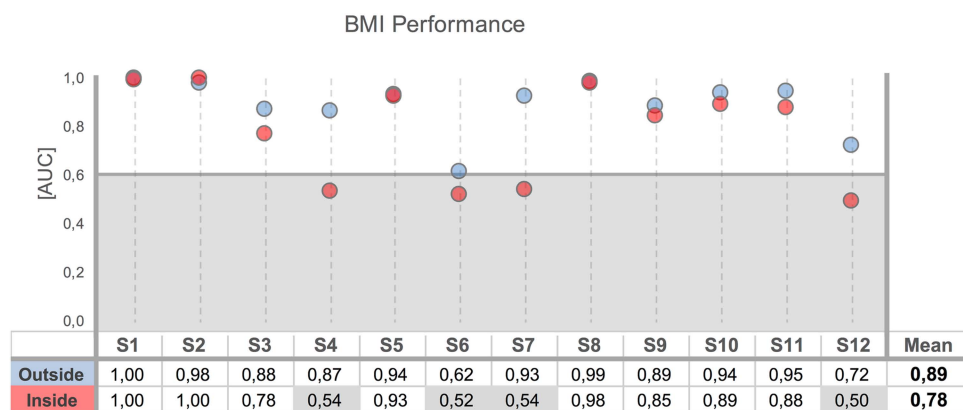


**Figure 4.**

BMI-control performance inside and outside of the MRI scanner. Single-subject BMI-control performance are shown for the session outside (training session, blue dots) and inside (BMI-fMRI session, red dots) the MRI scanner. The gray area indicates

performance that did not exceed the empirical chance threshold of 0.61: out of a total of 12 subjects, 4 participants did not perform above chance during the BMI-fMRI session. [Color figure can be viewed at [wileyonlinelibrary.com](http://wileyonlinelibrary.com)]

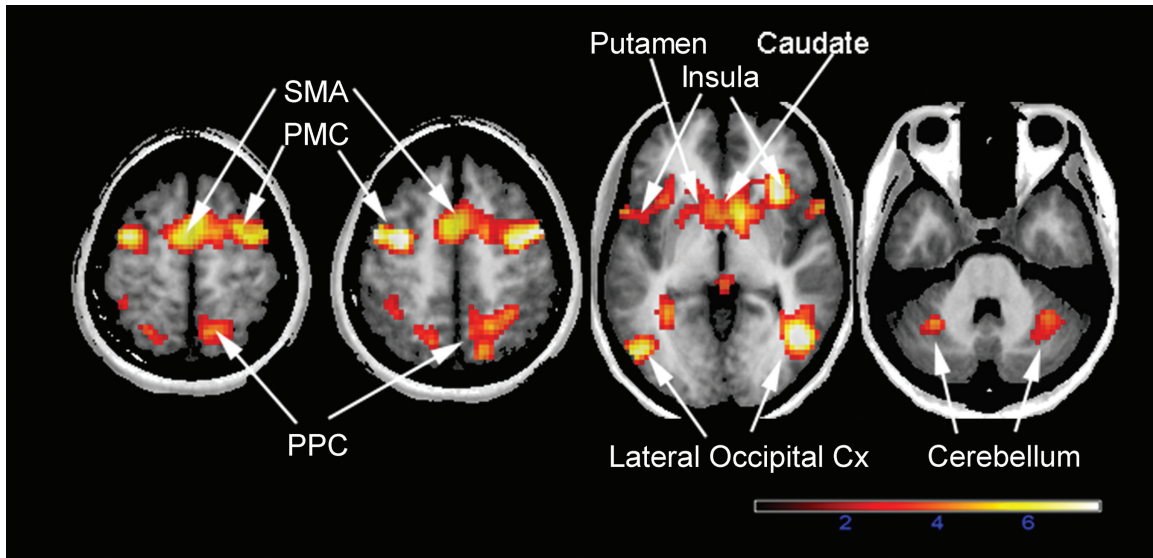


**Figure 5.**

BMI-related BOLD response. Group results showing the average brain response to the four experimental conditions irrespectively of the cue direction and of the movement manipulation ( $P < 0.05$  FDR).

**fMRI Data: Brain Regions Activated during BMI Control and in Comparison to Those of MI**

The results of the fMRI analysis investigating the regions involved in online BMI control revealed an

extended brain network that not only involved predominantly the sensorimotor regions but also included areas not reported before as being recruited during MI or BMI (Fig. 5). The experimental conditions were found to activate (thresholded at  $q < 0.05$  FDR corrected) a large

**TABLE II. Activations during BMI control**

Cluster number	Cluster size (voxels)	Peak	MNI Coordinates (mm)			Anatomical location
		<i>T</i>	<i>x</i>	<i>y</i>	<i>z</i>	
1	5638	9.78	-36	-4	52	Left Precentral Gyrus
		8.94	45	-67	1	Right LOC
		8.82	48	-1	55	Right Middle Frontal Gyrus
		8.12	33	20	4	Right Anterior Insula Lobe
		7.44	-48	-73	4	Left LOC
		7.06	36	-7	55	Right Precentral Gyrus
		6.71	57	-34	22	Right Superior Temporal Gyrus (TPJ)
		6.69	33	-1	67	Right Superior Frontal Gyrus
		6.62	12	8	-2	Right caudate nucleus
		6.21	-3	-4	58	Supplementary motor area
		6.18	-60	8	13	Left Frontal Operculum
		5.61	-33	17	10	Left Anterior Insula Lobe
		5.29	54	11	16	Right Frontal Operculum
		5.05	-6	8	-2	Left caudate nucleus
2	118	3.44	-21	11	1	Left Putamen
		4.78	36	-61	-29	Right Cerebellum - Crus I (Hem)
		4.03	27	-67	-26	Right Cerebellum - Lobule VI (Hem)
3	41	4.62	-33	-55	-32	Left Cerebellum - Lobule VI (Hem)
4	103	4.2	-15	-67	55	Left Superior Parietal Lobule
5	33	3.87	-15	-70	-23	Left Cerebellum - Lobule VI (Hem)
		3.77	-3	-79	-17	Left Cerebellum - Lobule VI (Vermis)
6	97	3.5	-39	-43	58	Left Superior Parietal Lobule

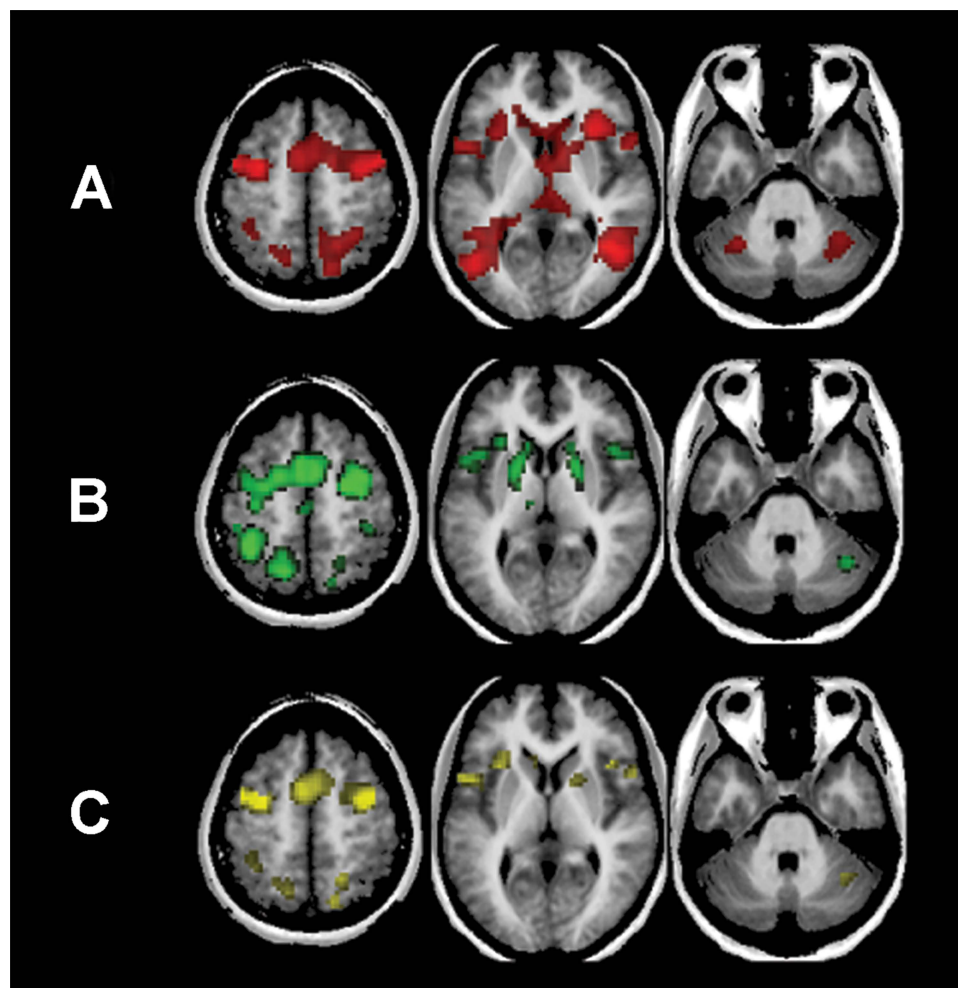


**Figure 6.**

Comparison between BMI-activity and MI meta-analysis results. **(A)** Activation found considering the positive effect of all experimental conditions ( $P < 0.05$  FDR, red). **(B)** Results from the meta-analysis on hand motor imagery ( $P < 0.05$  FDR, green). **(C)** Overlap between the two contrasts (yellow). [Color figure can be viewed at [wileyonlinelibrary.com](http://wileyonlinelibrary.com)]

network consisting of the bilateral premotor cortex (PMC) and primary motor cortex (M1), SMA, bilateral superior parietal cortex, bilateral frontal operculum, right superior temporal gyrus, bilateral anterior insula, bilateral lateral occipital cortex (LOC), and cerebellum. In addition, the bilateral caudate nucleus and left putamen were also activated by the BMI control task with respect to rest. The stereotaxic coordinates of the maxima of each activated cluster are reported in Table II. These data show that strong activations were not only observed in expected motor and premotor areas but also that several different areas outside motor cortex were involved in BMI control.

To compare the brain regions associated with online BMI control (Figs. 5 and 6A) with those reported during MI, we conducted a meta-analysis of 21 neuroimaging studies (Table I) that used hand MI paradigms (and were

thus comparable to the MI paradigm used in the present study, although the exact task instructions and requirements differed among these studies and with respect to the present BMI study). This meta-analysis of hand MI revealed activation of the bilateral SMA, the PMC, the primary motor and somatosensory cortices, the bilateral frontal operculum, the bilateral superior and inferior parietal lobule, middle cingulate cortex, bilateral insula, bilateral putamen, caudate and pallidum, left thalamus, and cerebellum (Fig. 6B, Table III). Directly comparing both datasets (present data on BMI control; MI data from meta-analysis) we found common activations (Fig. 6C) in many, but not all, regions activated during BMI control. Commonly activated were the bilateral PMC, SMA, bilateral frontal operculum, bilateral insula, bilateral superior parietal lobule, left inferior parietal lobe, right and left putamen, right

**TABLE III. Significant clusters identified by the ALE meta-analysis of neuroimaging studies of hand motor imagery**

Cluster number	Cluster size (vox)	MNI coordinates (mm)			ALE ( $\times 10^3$ )	Anatomical location
		<i>x</i>	<i>y</i>	<i>z</i>		
1	5493	-1	0	59	63.61	Supplementary motor area
		-38	-49	59	57.43	Left Inferior Parietal Lobule
		-21	-4	61	54.43	Left Superior Frontal Gyrus
		-56	5	30	40.50	Left Inferior Frontal Gyrus (p. Opercularis)
2	792	29	-7	55	53.61	RightPrecentral Gyrus
3	554	38	-32	44	39.81	Right Postcentral Gyrus
4	482	-19	-62	58	32.40	Left Superior Parietal Lobule
5	391	52	13	13	32.46	Right Inferior Frontal Gyrus (p. Opercularis)
6	378	-22	-1	4	26.46	Left Pallidum
		-26	-5	13	26.20	Left Putamen
		-10	19	8	17.26	Left Caudate Nucleus
7	287	20	6	9	27.53	Right Putamen
		22	0	3	24.09	Right Pallidum
		16	18	8	16.63	Right Caudate Nucleus
8	239	21	-59	60	27.64	Right Superior Parietal Lobule
		17	-73	52	21.73	Right Precuneus
9	149	-1	-23	49	28.63	Left Middle Cingulate Cortex
10	108	40	-58	-36	28.38	Right Cerebellum - Crus I
12	74	-61	-31	29	24.59	Left Inferior Parietal Gyrus
13	62	-30	-53	-17	17.89	Left Cerebellum - Lobule VI
14	59	-30	21	6	21.55	Left Insula Lobe
15	54	10	-66	-16	23.43	Right Cerebellum - Lobule VI
16	40	22	-57	-20	18.31	Right Cerebellum - Lobule VI
17	39	66	-37	30	20.26	Right Inferior Parietal Lobe
18	31	56	18	-13	20.43	Right Temporal Pole
19	28	-11	-19	9	17.45	Left Thalamus
20	20	-48	-64	-4	18.03	Left Inferior Temporal Gyrus
22	17	-40	-69	-28	18.69	Left Cerebellum - Crus I
25	16	-6	-48	-18	18.31	Left Cerebellum - I-IV
27	14	-2	-46	-4	16.70	Cerebellar Vermis

caudate, and cerebellum. The bilateral lateral occipital complex and the right supramarginal gyrus were only activated during online BMI control, whereas the thalamus was found only during hand MI (meta-analysis). These data provide additional evidence that the present participants relied on MI to perform BMI while in the scanner.

### fMRI Data: Right versus Left BMI Control

To determine which brain regions were differentially activated when attempting to move the cursor toward either the right or the left side of the screen, we contrasted the fMRI data associated with the right- versus those of the left-cued direction. This analysis revealed significant differences that were mainly restricted to the PMC, but also extended onto the primary motor cortex (Fig. 7A,  $q < 0.05$  FDR corrected). More specifically, when participants were asked to perform right MI we found a significantly stronger response in the left motor and premotor cortex, and similarly left MI was associated with a stronger activation in the same, but contralateral, motor cortices. Furthermore, we note that the cluster contralateral to the direction of cursor control showed relatively enhanced activation, whereas the

ipsilateral cluster showed relatively decreased activation (Fig. 7B). More detailed analysis of the anatomical location of these clusters revealed that cursor control primarily activated the contralateral PMC and, to a lesser extent, the contralateral primary motor cortex. The only other region that exhibited differential activation during right versus left cursor control was the cerebellum, showing a significantly stronger activation in the right cerebellum during right control. Additionally, by considering a more liberal threshold ( $P < 0.001$  uncorrected) when contrasting left versus right imagery, we observed a stronger activation in the left cerebellum (contralateral to the above-mentioned cluster in the right cerebellum).

### fMRI Data: Brain Regions Associated with Subjective Feelings of BMI Control (Sense of Agency)

Differences in the feeling of control over the cursor movement between *undeviated* and *deviated* trials were assessed with a two-tailed *t*-test. In accordance with previous BMI agency work from our laboratory (carried out outside the

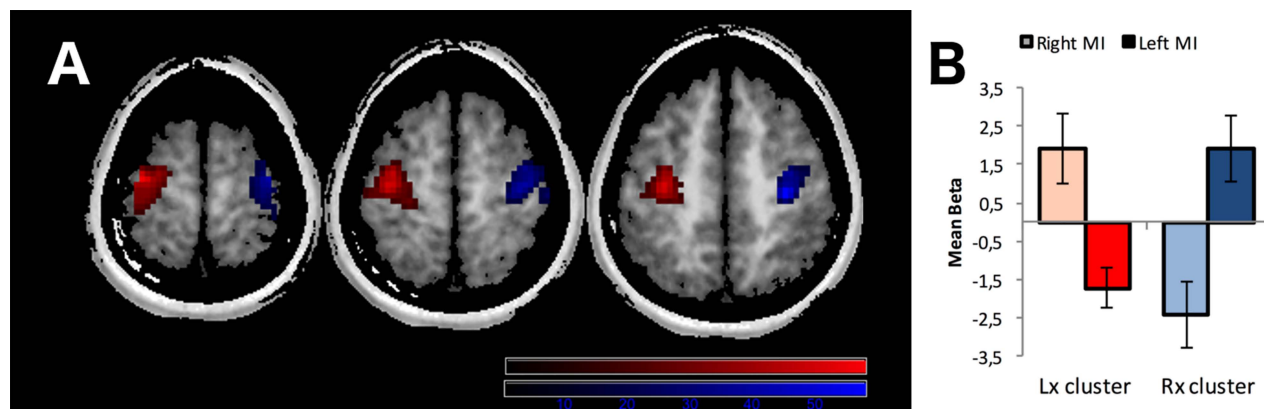


Figure 7.

Lateralized BMI activations. (A) Group results showing the effect of the cue-direction ( $P < 0.05$  FDR) over premotor and motor regions. The cluster over the left hemisphere (red) shows a higher activation during right MI whereas a stronger activity due to left MI is depicted in the cluster over the right

hemisphere (blue). (B) Mean beta values over the two clusters and for the two imagined directions. The hemisphere contralateral to the imagined direction shows a positive mean beta value, whereas the ipsilateral hemisphere is associated with a negative value. [Color figure can be viewed at [wileyonlinelibrary.com](http://wileyonlinelibrary.com)]

fMRI scanner) [Evans et al., 2015], we found that participants reported a significantly reduced SoA when the cursor trajectory was deviated (two-tailed paired  $t$ -test,  $t = 3.57$ ,  $P < 0.005$ ). Correlation analysis between BMI performance and agency judgements revealed a significant positive correlation for *undeviated* trials ( $r = 0.8672$ ,  $P < 0.0001$ ) and a

significant negative correlation for *deviated* trials ( $r = -0.8911$ ,  $P < 0.0001$ ), as expected.

To investigate the brain mechanisms associated with the SoA, we performed a statistical analysis with the within-subjects factors “cue direction” (left/right) and “feeling of control” (YES/NO). The main effect of the reported SoA revealed significantly

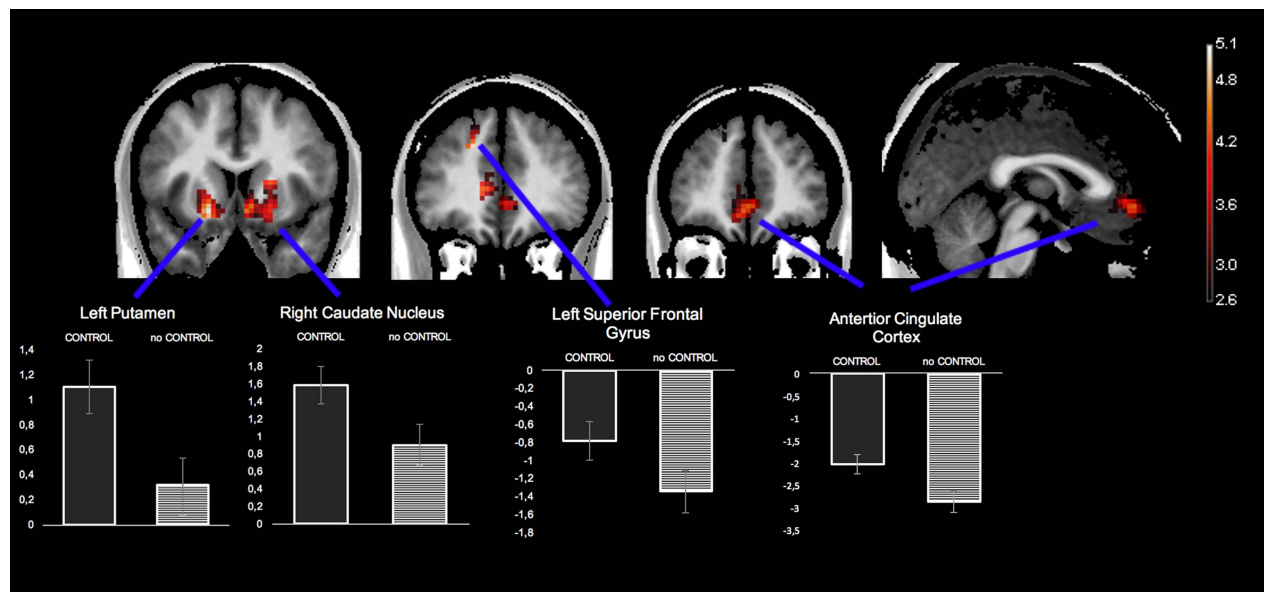


Figure 8.

Brain activity associated to the sense of agency for BMI control. Group results showing regions with stronger activations ( $P < 0.05$  FDR, masked with Any Effect contrast at  $P < 0.001$ ) when subjects reported feeling in control as opposed to not feeling in control. The activity over the basal ganglia region was

associated with positive BOLD response, unlike the one over the ACC and the left superior frontal gyrus, which showed a negative response to the stimulation. [Color figure can be viewed at [wileyonlinelibrary.com](http://wileyonlinelibrary.com)]

stronger activation in the caudate nucleus bilaterally and in the right putamen for those trials where subjects reported the feeling of being in control over the cursor movement (SoA), independently from the cue direction and the experimental manipulation ( $q < 0.05$  FDR masked with Any Effect contrast at  $P < 0.001$ , clusters with a spatial extent of at least 30 contiguous voxels, Fig. 8). Additionally, we found significant clusters located in the anterior cingulate cortex (ACC) and the left superior frontal gyrus. Follow-up analyses revealed that the neural activity over these two areas was associated with a negative BOLD response, unlike the activity over the above-mentioned basal ganglia region. There were no clusters showing stronger activation when subjects reported not feeling in control of the cursor compared to when they did.

## DISCUSSION

Using simultaneous EEG-fMRI, we were able to uncover the cortical and subcortical brain regions associated with different aspects of BMI control. Our paradigm allowed participants to control the movement of a visual cursor inside an MRI scanner, as confirmed by the average BMI-control performance being significantly above chance and further corroborated by the classical lateralized  $\mu$ -rhythm suppression being observed over premotor/motor scalp regions. We have organized our discussion around the three main goals of our study: (1) identify the network of regions involved in BMI control at the whole-brain level and (2) assess the overlap of these regions with those already reported as being recruited during pure MI; (3) uncover the neural correlates of the sense agency for BMI actions.

### Regions Active during BMI-Control

Regarding the first of our three hypotheses, we found bilateral premotor and primary motor cortex and, extending beyond these areas, we observed several other cortical structures, along with basal ganglia and cerebellum. Most EEG-based BMI approaches generally record data over a specific region of the scalp. For example, MI BMIs commonly decode brain signals from electrodes centered over motor cortex [Hochberg et al., 2012; Pfurtscheller and Neuper, 2001; Wolpaw and McFarland, 2004]. Similarly, a recent neuroimaging study of BMI provided EEG-based feedback while participants were inside the MRI scanner, but restricted the analysis to cortical premotor and motor regions [Zich et al., 2015]. By contrast our approach allowed us to investigate the network associated with BMI control across the entire brain. The premotor and motor areas that we report in the present study (PMC, M1, SMA) have been consistently reported during MI tasks [Jeanerod, 2001; Lotze and Halsband, 2006] and these regions have been associated with cortical reorganization during learning to control a BMI [Carmena et al., 2003].

In addition to sensorimotor regions, our data also revealed an involvement of the posterior parietal cortex

(PPC) as well as insular cortex. Decoding PPC activity has been used for high-level aspects of action planning, which can be translated into the control of trajectories and goals of external devices [i.e., Aflalo et al., 2015]. Furthermore, activity in PPC was found to be modulated by the acquisition of expertise in BMI-control [Wander et al., 2013]. Less is known about the insula's involvement in BMI control: previous studies have shown that subjects can successfully control this area using real-time fMRI-based neurofeedback [Caria et al., 2007]. We argue that its activation in our paradigm underlies its hub-like role in integrating sensorimotor signals due to its strong connection with motor and premotor areas [Cauda et al., 2011], and its involvement in MI [Hétu et al., 2013; Sacco et al., 2006; Solodkin et al., 2004]. The cerebellum and the basal ganglia also showed marked activation during on-line BMI control. An extensive body of literature has focused on the importance of these structures for motor control [Graybiel et al., 1994] and MI [Decety et al., 1994; Dominey et al., 1995; Guillot et al., 2008; Jeanerod, 2001]. For example, damage to the cerebellum has been reported to impair MI [Battaglia et al., 2006].

Only three regions—bilateral PMC, M1, and cerebellum—exhibited differential activation for rightward versus leftward cursor control. In line with results from a previous study that used a similar experimental set-up [Zich et al., 2015], BMI control of the cursor to either the right or the left side was reflected in stronger activation of a cluster overlapping the contralateral PMC. The present data show that the same is true, albeit to a lesser degree, for M1. Although M1 recruitment in MI is controversial, electrocorticographic (ECoG) recordings have shown prominent M1 activation during MI-based BMI compared to MI without feedback [Miller et al., 2010] and activation in M1 has also been associated with expertise in MI [Sharma et al., 2008]. The present data support the involvement of M1 in MI-based BMI control. In line with previous studies [Yuan et al., 2010; Zich et al., 2015], we also observed the negative relationship between beta values in PMC and M1 regions and the  $\mu$ -band suppression in the EEG over the same areas.

Interestingly, additional differences between right- and left-hand MI were found in the cerebellum, associating right MI with ipsilateral right cerebellar activation and left MI with ipsilateral left cerebellar activation (although the latter activation did not reach significance after correction for multiple comparisons). None of the other regions found to be active during BMI-control discriminated between left and right hand MI, suggesting that these regions reflect more basic differences with respect to the control condition as in non-lateralized MI, visual stimulation, or other cognitive aspects of BMI control such as action planning.

### Common and Distinct Brain Activations during Motor-Imagery and BMI-Control

Regarding our second hypothesis (i.e., an overlap of the activations previously described with those reported for

MI), we performed a meta-analysis of a large sample of brain-imaging studies aimed at investigating which of these regions associated with MI-based BMI control were also recruited during hand MI. As hypothesized, we found several brain regions common to both tasks (MI and on-line BMI control) including PMC, M1, and SMA as well as PPC, insula, and cerebellum. However, we also observed that BMI-control recruited additional regions in lateral occipital cortex that overlapped with coordinates of the extrastriate body area, a region reported to be activated during MI as well as visual feedback with respect to ongoing movements [i.e., Astafiev et al., 2004; Arzy et al., 2006; Ninaus et al., 2013].

### Sense of Agency for BMI Control

Human action is associated with a SoA, the feeling that one's movements and their consequences are self-generated and not externally produced [David et al., 2008; Gallagher, 2000; Pacherie, 2008] and this has been investigated in behavioral [Fournier et al., 1998; Tsakiris and Haggard, 2005] and neuroimaging studies [David et al., 2007; Farrer et al., 2003; Farrer and Frith, 2002]. Based on a recent behavioral study, we experimentally manipulated the visual feedback in half of the trials, by inverting the cursor movement direction with respect to the decoded one. In this context, our third hypothesis consisted of observing the coactivation of regions previously associated with the SoA for bodily actions, together with regions specific for BMI-mediated action. More specifically, Evans et al. showed that the SoA for BMI-mediated actions largely relies on the matching between intentions and the sensory outcome (i.e., the visual feedback) [Evans et al., 2015].

The present behavioral data confirm previous findings obtained using a similar EEG-BMI system [Evans et al., 2015] and reveal that the SoA for such actions is stronger for *undeviated* trials. We also report stronger activation in subcortical structures (caudate nucleus, putamen) in trials with a high SoA. A previous BMI-fMRI study indicated that caudate nucleus and putamen contribute critically to successful control in self-regulation tasks [Hinterberger et al., 2005]. We extend those findings by showing that these regions contribute also to the subjective sense of BMI control. In addition, we note that the putamen has previously been implicated in the SoA for executed actions [i.e., Leube, 2003] and that SoA disturbances have been associated with pathological conditions affecting dopaminergic transmission in the caudate nucleus such as Parkinson disease [Bramley and Eatough, 2005]. Our data also linked the SoA during BMI control to the ACC, a region that has previously been linked to the SoA for bodily movements [Farrer et al., 2003]. We note that Farrer et al. exposed participants to spatio-temporal conflicts between the expected and actual visual feedback, similar to our paradigm. However, while previous studies tested the SoA for physical actions characterized by a high

degree of automaticity, "BMI-actions" are learned actions and require a high degree of attention and cognitive control. In light of this, it is worth noting that ACC activity is suppressed when participants acquire an automatic response through learning, while it is activated when participants are instructed to think about their own motor performance [Jueptner et al., 1997; Lau et al., 2004]. Last, it should be noted that the activity over basal ganglia together with that over ACC suggest the involvement of mechanisms of reward processing. Dopamine neurons in the basal ganglia code for error detection in reward prediction [Doya, 2000; Schultz et al., 2000] and in line with this predictive role, it has been shown that activity in the putamen and caudate is increased when stimulus-outcome contingencies are learned [Seger and Cincotta, 2005]. Similarly, the ACC is known as a key structure for conflict monitoring [Botvinick et al., 2004; Van Veen and Carter, 2002], error-processing [Menon et al., 2001], and reward signals [Bush et al., 2002].

### CONCLUSION

Our results reveal an extended network involved in BMI control, and point to distinct contributions of different cortico-subcortical components enabling MI based BMI including lateralized control, and the subjective sense of being in control (i.e., the SoA). Our results on the SoA may contribute to the development of BMI systems that allow a more natural experience of feeling in control and point to the importance of "biomimicry," that is, the artificial reproduction of natural conditions happening during movements in BMI systems [Perruchoud et al., 2016]. In this context, it would be important to determine which aspect of sensory feedback contributes to BMI control. This is worthy of note considering recent results showing that when no on-line feedback is provided, learning of self-performance monitoring is delayed [Schurger et al., 2017]. With respect to BMI control, our findings show that while signals recorded from motor and premotor areas via scalp electrodes are sufficient for delivering command signals, a much larger and distributed cortical-subcortical network of brain regions is also involved, including the cerebellum, the lateral occipital cortex, and the basal ganglia. Future work should be directed at uncovering which aspect of BMI control each region of this network contributes to, notably in terms of learning [Koralek et al., 2012, 2013], achieving [Marchesotti et al., 2016], and maintaining the control over BMI-mediated actions.

### ACKNOWLEDGMENTS

The authors thank Nathan Evans and Ulrike Toepel for the helpful discussions and advices.

## CONFLICT OF INTEREST

All authors report no potential conflicts of interest.

## REFERENCES

- Aflalo T, Kellis S, Klaes C, Lee B, Shi Y, Pejsa K, Shanfield K, Hayes-Jackson S, Aisen M, Heck C, Liu C, Andersen RA (2015): Decoding motor imagery from the posterior parietal cortex of a tetraplegic human. *Science* (80-) 348:906–910.
- Allen PJ, Josephs O, Turner R (2000): A method for removing imaging artifact from continuous EEG recorded during functional MRI. *Neuroimage* 12:230–239.
- Arzy S, Thut G, Mohr C, Michel CM, Blanke O (2006): Neural basis of embodiment: distinct contributions of temporoparietal junction and extrastriate body area. *J Neurosci* 26:8074–81.
- Astafiev S V, Stanley CM, Shulman GL, Corbetta M (2004): Extrastriate body area in human occipital cortex responds to the performance of motor actions. *Nat Neurosci* 7:542–8.
- Battaglia F, Quartarone A, Ghilardi MF, Dattola R, Bagnato S, Rizzo V, Morgante L, Girlanda P (2006): Unilateral cerebellar stroke disrupts movement preparation and motor imagery. *Clin Neurophysiol* 117:1009–1016.
- Blankertz B, Tomioka R, Lemm S, Kawanabe M, Muller K (2008): Optimizing spatial filters for robust EEG single-trial analysis. *IEEE Signal Process Mag* 25:41–56.
- Binkofski F, Amunts K, Stephan KM, Posse S, Schormann T, Freund HJ, Zilles K, Seitz RJ (2000): Broca’s region subserves imagery of motion: a combined cytoarchitectonic and fMRI study. *Hum Brain Mapp* 11:273–85.
- Boecker H, Ceballos-Baumann AO, Bartenstein P, Dagher A, Forster K, Haslinger B, Brooks DJ, Schwaberg M, Conrad B (2002): A H(2)(15)O positron emission tomography study on mental imagery of movement sequences—the effect of modulating sequence length and direction. *Neuroimage* 17:999–1009.
- Botvinick MM, Cohen JD, Carter CS (2004): Conflict monitoring and anterior cingulate cortex: An update. *Trends Cogn Sci* 8: 539–546.
- Bramley N, Eatough V (2005): The experience of living with Parkinson’s disease: An interpretative phenomenological analysis case study. *Psychol Health* 20:223–235.
- Bush G, Vogt B a, Holmes J, Dale AM, Greve D, Jenike M a, Rosen BR (2002): Dorsal anterior cingulate cortex: a role in reward-based decision making. *Proc Natl Acad Sci U S A* 99: 523–528.
- Caria A, Veit R, Sitaram R, Lotze M, Weiskopf N, Grodd W, Birbaumer N (2007): Regulation of anterior insular cortex activity using real-time fMRI. *Neuroimage* 35:1238–1246.
- Carmena JM, Lebedev MA, Crist RE, O’Doherty JE, Santucci DM, Dimitrov DF, Patil PG, Henriquez CS, Nicolelis M. a L (2003): Learning to control a brain-machine interface for reaching and grasping by primates. *PLoS Biol* 1:E42.
- Cauda F, D’Agata F, Sacco K, Duca S, Geminiani G, Vercelli A (2011): Functional connectivity of the insula in the resting brain. *Neuroimage* 55:8–23.
- Combrisson E, Jerbi K (2015): Exceeding chance level by chance: The caveat of theoretical chance levels in brain signal classification and statistical assessment of decoding accuracy. *J Neurosci Methods* 250:126–136.
- Creem-Regehr SH, Lee JN (2005): Neural representations of graspable objects: are tools special? *Brain Res Cogn Brain Res* 22: 457–69.
- David N, Cohen MX, Newen A, Bewernick BH, Shah NJ, Fink GR, Vogeley K (2007): The extrastriate cortex distinguishes between the consequences of one’s own and others’ behavior. *Neuroimage* 36:1004–1014.
- David N, Newen A, Vogeley K (2008): The “sense of agency” and its underlying cognitive and neural mechanisms. *Conscious Cogn* 17:523–534.
- Decety J (1996): The neurophysiological basis of motor imagery. *Behav Brain Res* 77:45–52.
- Decety J, Perani D, Jeannerod M, Bettinardi V, Tadary B, Woods R, Mazziotta JC, Fazio F (1994): Mapping motor representations with positron emission tomography. *Nature* 371:600–602.
- Dominey P, Decety J, Broussolle E, Chazot G, Jeannerod M (1995): Motor imagery of a lateralized sequential task is asymmetrically slowed in hemi-Parkinson’s patients. *Neuropsychologia* 33:727–741.
- Doya K (2000): Complementary roles of basal ganglia and cerebellum in learning and motor control. *Curr Opin Neurobiol* 10: 732–739.
- Ehrsson HH, Geyer S, Naito E (2003): Imagery of voluntary movement of fingers, toes, and tongue activates corresponding body-part-specific motor representations. *J Neurophysiol* 90: 3304–3316.
- Eickhoff SB, Laird AR, Grefkes C, Wang LE, Zilles K, Fox PT (2009): Coordinate-based activation likelihood estimation meta-analysis of neuroimaging data: A random-effects approach based on empirical estimates of spatial uncertainty. *Hum Brain Mapp* 30:2907–2926.
- Evans N, Gale S, Schurger A, Blanke O (2015): Visual feedback dominates the sense of agency for brain-machine actions. *PLoS One* 10:e0130019.
- Farrer C, Frith CD (2002): Experiencing oneself vs another person as being the cause of an action: The neural correlates of the experience of agency. *Neuroimage* 15:596–603.
- Farrer C, Franck N, Georgieff N, Frith CD, Decety J, Jeannerod M (2003): Modulating the experience of agency: A positron emission tomography study. *Neuroimage* 18:324–333.
- Fetz EE (1969): Operant conditioning of cortical unit activity. *Science* (80-) 163:955–958.
- Filimon F, Nelson JD, Hagler DJ, Sereno MI (2007): Human cortical representations for reaching: mirror neurons for execution, observation, and imagery. *Neuroimage* 37:1315–28.
- Fournier P, Jeannerod M (1998): Limited conscious monitoring of motor performance in normal subjects. *Neuropsychologia* 36: 1133–1140.
- Friston KJ, Holmes AP, Worsley KJ, Poline J-P, Frith CD, Frackowiak RSJ (1994): Statistical parametric maps in functional imaging: A general linear approach. *Hum Brain Mapp* 2: 189–210.
- Gallagher I (2000): Philosophical conceptions of the self: Implications for cognitive science. *Trends Cogn Sci* 4:14–21.
- Gerardin E, Sirigu a, Lehericy S, Poline JB, Gaymard B, Marsault C, Agid Y, Le Bihan D (2000): Partially overlapping neural networks for real and imagined hand movements. *Cereb Cortex* 10:1093–104.
- Grafton ST, Arbib MA, Fadiga L, Rizzolatti G (1996): Localization of grasp representations in humans by positron emission tomography. *Experimental Brain Research*. 112:103–111
- Graybiel A, Aosaki T, Flaherty A, Kimura M (1994): The basal ganglia and adaptive motor control. *Science* (80-) 265:1826–1831.
- Guger C, Ramoser H, Pfurtscheller G (2000): Real-time EEG analysis with subject-specific spatial patterns for a brain-computer interface (BCI). *IEEE Trans Rehabil Eng* 8:447–456.

- Guillot A, Collet C, Nguyen VA, Malouin F, Richards C, Doyon J (2008): Functional neuroanatomical networks associated with expertise in motor imagery. *Neuroimage* 41:1471–1483.
- Halder S, Agorastos D, Veit R, Hammer EM, Lee S, Varkuti B, Bogdan M, Rosenstiel W, Birbaumer N, Kübler A (2011): Neural mechanisms of brain-computer interface control. *Neuroimage* 55:1779–1790.
- Hanakawa T, Dimyan M a, Hallett M (2008): Motor planning, imagery, and execution in the distributed motor network: a time-course study with functional MRI. *Cereb Cortex* 18:2775–88.
- Harrington GS, Farias D, Davis CH, Buonocore MH (2007): Comparison of the neural basis for imagined writing and drawing. *Hum Brain Mapp* 28:450–9.
- Héту S, Grégoire M, Saimpont A, Coll M-P, Eugène F, Michon P-E, Jackson PL (2013): The neural network of motor imagery: An ALE meta-analysis. *Neurosci Biobehav Rev* 37:930–949.
- Hinterberger T, Veit R, Wilhelm B, Weiskopf N, Vatine J-J, Birbaumer N (2005): Neuronal mechanisms underlying control of a brain-computer interface. *Eur J Neurosci* 21:3169–3181.
- Hochberg LR, Bacher D, Jarosiewicz B, Masse NY, Simeral JD, Vogel J, Haddadin S, Liu J, Cash SS, van der Smagt P, Donoghue JP (2012): Reach and grasp by people with tetraplegia using a neurally controlled robotic arm. *Nature* 485:372–375.
- Jarosiewicz B, Chase SM, Fraser GW, Velliste M, Kass RE, Schwartz AB (2008): Functional network reorganization during learning in a brain-computer interface paradigm. *Proc Natl Acad Sci USA* 105:19486–19491.
- Jeannerod M (2001): Neural simulation of action: A unifying mechanism for motor cognition. *Neuroimage* 14:S103–S109.
- Johnson SH, Rotte M, Grafton ST, Hinrichs H, Gazzaniga MS, Heinze HJ (2002): Selective activation of a parietofrontal circuit during implicitly imagined prehension. *Neuroimage* 17:1693–704.
- Jueptner M, Ottinger S, Fellows SJ, Adamschewski J, Flerich L, Müller SP, Diener HC, Thilmann AF, Weiller C (1997): The relevance of sensory input for the cerebellar control of movements. *Neuroimage* 5:41–48.
- Koralek AC, Jin X, Long JD, Costa RM, Carmena JM (2012): Corticostriatal plasticity is necessary for learning intentional neuroprosthetic skills. *Nature* 483:331–335.
- Koralek AC, Costa RM, Carmena JM (2013): Temporally precise cell-specific coherence develops in corticostriatal networks during learning. *Neuron* 79:865–872.
- Kuhtz-Buschbeck JP, Mahnkopf C, Holzknrecht C, Siebner H, Ulmer S, Jansen O (2003): Effector-independent representations of simple and complex imagined finger movements: A combined fMRI and TMS study. *Eur J Neurosci* 18:3375–3387.
- Lacourse MG, Orr ELR, Cramer SC, Cohen MJ (2005): Brain activation during execution and motor imagery of novel and skilled sequential hand movements. *Neuroimage* 27:505–19.
- Laird AR, Fox PM, Price CJ, Glahn DC, Uecker AM, Lancaster JL, Turkeltaub PE, Kochunov P, Fox PT (2005): ALE meta-analysis: Controlling the false discovery rate and performing statistical contrasts. *Hum Brain Mapp* 25:155–164.
- Laird AR, Eickhoff SB, Kurth F, Fox PM, Uecker AM, Turner JA, Robinson JL, Lancaster JL, Fox PT (2009): ALE meta-analysis workflows via the brainmap database: Progress towards a probabilistic functional brain atlas. *Front Neuroinform* 3:23.
- Lamm C, Fischer MH, Decety J (2007): Predicting the actions of others taps into one's own somatosensory representations—a functional MRI study. *Neuropsychologia* 45:2480–91.
- Lau HC, Rogers RD, Haggard P, Passingham RE (2004): Attention to intention. *Science* 303:1208–1210.
- Leeb R, Perdakis S, Tonin L, Biasucci A, Tavella M, Creatura M, Molina A, Al-Khodairy A, Carlson T, Millán JDR (2013): Transferring brain-computer interfaces beyond the laboratory: Successful application control for motor-disabled users. *Artif Intell Med* 59:121–132.
- Leube D (2003): The neural correlates of perceiving one's own movements. *Neuroimage* 20:2084–2090.
- Lipnicki DM (2009): Baroreceptor activity potentially facilitates cortical inhibition in zero gravity. *Neuroimage* 46:10–11.
- Lotze M, Halsband U (2006): Motor imagery. *J Physiol Paris* 99:386–395.
- Makeig S (1993): Auditory event-related dynamics of the EEG spectrum and effects of exposure to tones. *Electroencephalogr Clin Neurophysiol* 86:283–293.
- Marchesotti S, Bassolino M, Serino A, Bleuler H, Blanke O (2016): Quantifying the role of motor imagery in brain-machine interfaces. *Sci Rep* 6:24076.
- Marques JP, Kober T, Krueger G, van der Zwaag W, Van de Moortele P-F, Gruetter R (2010): MP2RAGE, a self bias-field corrected sequence for improved segmentation and T1-mapping at high field. *Neuroimage* 49:1271–1281.
- McFarland DJ, Miner LA, Vaughan TM, Wolpaw JR (2000): Mu and beta rhythm topographies during motor imagery and actual movements. *Brain Topogr* 12:177–186.
- Menon V, Adelman NE, White CD, Glover GH, Reiss AL (2001): Error-related brain activation during a Go/NoGo response inhibition task. *Hum Brain Mapp* 12:131–143.
- Millán JDR, Rupp R, Müller-Putz GR, Murray-Smith R, Giugliemma C, Tangermann M, Vidaurre C, Cincotti F, Kübler a, Leeb R, Neuper C, Müller K-R, Mattia D (2010): Combining brain-computer interfaces and assistive technologies: State-of-the-art and challenges. *Front Neurosci* 4:1–15.
- Miller KJ, Schalk G, Fetz EE, den Nijs M, Ojemann JG, Rao RPN (2010): Cortical activity during motor execution, motor imagery, and imagery-based online feedback. *Proc Natl Acad Sci USA* 107:4430–4435.
- Müller-Gerking J, Pfurtscheller G, Flyvbjerg H (1999): Designing optimal spatial filters for single-trial EEG classification in a movement task. *Clin Neurophysiol* 110:787–798.
- Müller-Putz GR, Scherer R, Brunner C, Leeb R, Pfurtscheller G (2008): Better than random? A closer look on BCI results. *Int J Bioelectromagn* 10:52–55.
- Neuper C, Müller-Putz GR, Scherer R, Pfurtscheller G (2006): Motor imagery and EEG-based control of spelling devices and neuroprostheses. *Prog Brain Res* 159:393–409.
- Ninaus M, Kober SE, Witte M, Koschutnig K, Stangl M, Neuper C, Wood G (2013): Neural substrates of cognitive control under the belief of getting neurofeedback training. *Front Hum Neurosci* 7:914.
- Pacherie E (2008): The phenomenology of action: A conceptual framework. *Cognition* 107:179–217.
- Perruchoud D, Pisotta I, Carda S, Murray MM, Ionta S (2016): Biometric rehabilitation engineering: The importance of somatosensory feedback for brain-machine interfaces. *J Neural Eng* 13:41001.
- Pfurtscheller G, Neuper C (1997): Motor imagery activates primary sensorimotor area in humans. *Neurosci Lett* 239:65–68.
- Pfurtscheller G, Neuper C (2001): Motor imagery and direct brain-computer communication. *Proc IEEE* 89:1123–1134.
- Pfurtscheller G, Neuper C, Flotzinger D, Pregezer M (1997): EEG-based discrimination between imagination of right and

- left hand movement. *Electroencephalogr Clin Neurophysiol* 103:642–651.
- Pfurtscheller G, Lopes da Silva FH (1999): Event-related EEG/MEG synchronization and desynchronization: Basic principles. *Clin Neurophysiol* 110:1842–1857.
- Rice JK, Rorden C, Little JS, Parra LC (2013): Subject position affects EEG magnitudes. *Neuroimage* 64:476–484.
- Sacco K, Cauda F, Cerliani L, Mate D, Duca S, Geminiani GC (2006): Motor imagery of walking following training in locomotor attention. The effect of “the tango lesson.” *Neuroimage* 32:1441–1449.
- Schultz W, Tremblay L, Hollerman JR (2000): Reward processing in primate orbitofrontal cortex and basal ganglia. *Cereb Cortex* 10:272–284.
- Schurger A, Gale S, Gozel O, Blanke O (2017): Performance monitoring for brain-computer-interface actions. *Brain Cogn* 111:44–50.
- Seger CA, Cincotta CM (2005): The roles of the caudate nucleus in human classification learning. *J Neurosci* 25:2941–2951.
- Seitz RJ, Stephan KM, Binkofski F (2000): Control of action as mediated by the human frontal lobe. *Exp Brain Res* 133:71–80.
- Servos P, Osu R, Santi A, Kawato M (2002): The neural substrates of biological motion perception: an fMRI study. *Cereb Cortex* 12:772–82.
- Sharma N, Jones PS, Carpenter TA, Baron J-C (2008): Mapping the involvement of BA 4a and 4p during Motor Imagery. *Neuroimage* 41:92–99.
- Solodkin A, Hlustik P, Chen EE, Small SL (2004): Fine modulation in network activation during motor execution and motor imagery. *Cereb Cortex* 14:1246–1255.
- Stephan KM, Fink GR, Passingham RE, Silbersweig D, Ceballos-Baumann AO, Frith CD, Frackowiak RS (1995): Functional anatomy of the mental representation of upper extremity movements in healthy subjects. *J Neurophysiol* 73:373–86.
- Szameitat AJ, Shen S, Sterr A (2007a): Motor imagery of complex everyday movements. An fMRI study. *Neuroimage* 34:702–13.
- Szameitat AJ, Shen S, Sterr A (2007b): Effector-dependent activity in the left dorsal premotor cortex in motor imagery. *Eur J Neurosci* 26:3303–8.
- Tsakiris M, Haggard P (2005): Experimenting with the acting self. *Cogn Neuropsychol* 22:387–407.
- Van Veen V, Carter C (2002): The anterior cingulate as a conflict monitor: fMRI and ERP studies. *Physiol Behav* 77:477–482.
- Wander JD, Blakely T, Miller KJ, Weaver KE, Johnson LA, Olson JD, Fetz EE, Rao RPN, Ojemann JG (2013): Distributed cortical adaptation during learning of a brain-computer interface task. *Proc Natl Acad Sci USA* 110:10818–10823.
- Wolpaw JR, McFarland DJ (2004): Control of a two-dimensional movement signal by a noninvasive brain-computer interface in humans. *Proc Natl Acad Sci USA* 101:17849–17854.
- Wolpaw JR, Birbaumer N, McFarland DJ, Pfurtscheller G, Vaughan TM (2002): Brain-computer interfaces for communication and control. *Clin Neurophysiol* 113:767–791.
- Yuan H, Liu T, Szarkowski R, Rios C, Ashe J, He B (2010): Negative covariation between task-related responses in alpha/beta-band activity and BOLD in human sensorimotor cortex: An EEG and fMRI study of motor imagery and movements. *Neuroimage* 49:2596–2606.
- Zich C, Debener S, Kranczioch C, Bleichner MG, Gutberlet I, De Vos M (2015): Real-time EEG feedback during simultaneous EEG–fMRI identifies the cortical signature of motor imagery. *Neuroimage* 114:438–447.